A Dynamic Bayesian Network Approach for Modeling High-Wind Probabilistic Safety Assessment in Nuclear Power Plants.

Chaeyeon Go[a], Shinyoung Kwag[b*], Seunghyun Eem[c], Changuk Mun[d], and Daegi Hahm[e]
[a]Hanbat National University, Daejeon, Republic of Korea, hocrosss25@gmail.coms
[b*] Hanbat National University, Daejeon, Republic of Korea, skwag@hanbat.ac.kr
[c] Kyungpook National University, Sangju, Republic of Korea, eemsh@knu.ac.kr
[d] Korea Atomic Energy Research Institute, Daejeon, Republic of Korea, changukmun@kaeri.re.kr
[e] Korea Atomic Energy Research Institute, Daejeon, Republic of Korea, dhahm@kaeri.re.kr

Abstract: High winds are external hazards that can affect the safety of nuclear power plants (NPPs), primarily through wind-borne debris and loss of offsite power. While Probabilistic Safety Assessment (PSA) methods based on Event Tree (ET) and Fault Tree (FT) models are widely used to evaluate such risks, they face inherent limitations in representing complex component dependencies and cascading failure effects. This study utilizes a Bayesian network (BN)-based approach for high-wind PSA. First, we develop an ET-FT scenario of high-wind-induced NPP. Then, it involves converting ET-FT models into a BN to enable probabilistic inference within a unified framework. Furthermore, to address the limitations of static BN models, this research introduces an intensity-based Dynamic Bayesian Network (DBN) in which system states evolve as a function of hazard intensity. This approach effectively captures component dependencies, accounts for cascading effects such as debris impact and power loss, supports data-driven probability updates, and enables system-level risk assessment across varying hazard intensities. The proposed DBN method is applied to a Korean OPR1000 reactor unit to demonstrate its applicability. The analysis results identify cascading failure scenarios and system-level risk transitions with varying hazard intensity, insights that are difficult to obtain with conventional static ET-FT models.

1. INTRODUCTION

Following the 2011 Fukushima accident, the need for systematic assessment of external hazard impacts on nuclear power plant (NPP) safety was emphasized, and regulatory bodies, including the USNRC, revised their guidelines to expand the scope of external-hazard PSA to cover earthquakes, floods, high winds, and other hazards [1]. Among external hazards, high winds can take various forms, including tornadoes, hurricanes (typhoons), and thunderstorms, and can directly damage NPP structures, systems, and components (SSCs) through wind-pressure loading, wind-borne missile impacts, and loss of offsite power (LOOP). Particularly, because high winds act across the entire plant site, they can cause simultaneous damage to multiple SSCs and cascading failures; accordingly, PSA for high-wind hazards is treated as a key component of external-hazard PSA [2].

Against this background, conventional high-wind PSA consists of three steps: hazard analysis, SSC fragility analysis, and plant response analysis [1, 3], following a methodological framework similar to seismic PSA. In each step, wind speed is set as the intensity measure; the SSC damage probability at each wind speed level is calculated using lognormal fragility curves; and the core damage frequency (CDF) is computed by convolving these with the wind hazard curve [4, 5]. Prior studies have identified LOOP as the dominant contributor to CDF [3], and wind-borne missile impacts are also considered a major damage pathway for NPP SSCs [5]. However, since this approach processes each wind-speed intensity level independently, it has limitations in explicitly modeling the cascading propagation of SSC

damage states as wind speed increases and the inter-SSC dependencies in cascading failure scenarios where wind-borne missile impact and LOOP act in combination.

To address these limitations, Bayesian network (BN)-based approaches have gained attention as alternatives to conventional ET-FT models. Unlike ET-FT models, BNs inherently support the representation of complex statistical dependencies among SSCs, Bayesian probabilistic inference, and uncertainty propagation [6, 7], and are well-suited for modeling cascading effects across multi-hazard scenarios within a unified framework [8, 9]. However, static BN approaches fix the system state at a single point in time, making it difficult to explicitly capture the dynamic transitions of SSC damage states and conditional probabilities as wind speed intensity varies. Dynamic Bayesian networks (DBNs) overcome this limitation of static BNs by modeling system behavior as a function of time or state changes. Nevertheless, an intensity-based DBN approach that uses wind-speed intensity as the state-transition axis to model the integrated propagation and dependencies among SSC damage states has not yet been presented. This study, therefore, proposes a methodology for applying intensity-based DBNs to high-wind PSA and demonstrates its applicability using a Korean OPR1000 reactor.

In this context, the study proposes an intensity-based DBN framework for high-wind external-hazard PSA of NPPs. The framework converts the ET-FT-based system model used in conventional high-wind PSA into a BN that represents accident scenarios and inter-SSC dependencies within a unified probabilistic inference structure. The key feature of this framework is reinterpreting the temporal index as wind intensity level rather than actual time, so the SSC damage state at a previous intensity level is reflected in the fragility and conditional probability table (CPT) at the subsequent intensity level. This enables damage-state propagation and adaptive risk evaluation as wind intensity increases within a single integrated framework. The proposed methodology is applied to a Korean OPR1000 reactor, and its validity is examined through case studies of damage-state scenarios.

2. METHOD

2.1. High Wind PSA Model

Figure 1: ET for High Wind-Induced Accident Scenarios

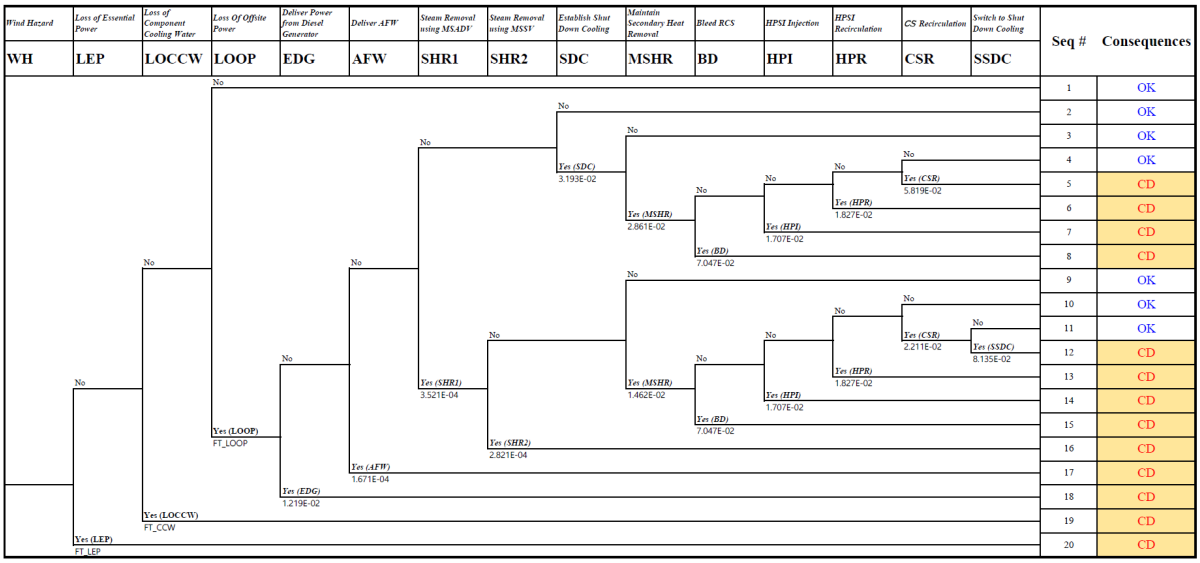

The Shin-Kori Units 1 and 2, both OPR1000 models, were selected as the target nuclear power plant (NPP) for a high-wind probabilistic safety assessment (PSA) in this study. The high-wind PSA involved four main steps: (1) hazard analysis to determine the annual exceedance frequency based on wind speed, (2) fragility analysis to estimate the damage probability of SSCs as a function of wind speed, (3) failure mode and effects analysis to evaluate how SSC damage affects systems and to construct the ET-FT for systems analysis, and (4) calculation of the core damage frequency (CDF) using the ET-FT. The hazard

analysis produced a hazard curve using an extreme-value distribution and wind-speed return-period data derived from the RCP8.5 scenario for the Busan region. The SSCs considered in the fragility analysis include the auxiliary building (AUX), EDG building, ESW intake structure building, CCW heat exchanger building, turbine building, and switchyard structure. Each SSC's fragility is represented by a lognormal fragility curve.

Three wind-induced initiating events are considered: loss of essential power (LEP), loss of component cooling water (LOCCW), and loss of offsite power (LOOP). LEP is initiated by damage to the auxiliary building or the EDG building, and LOCCW is initiated by damage to the ESW intake structure building or the CCW heat exchanger building. LEP and LOCCW are assumed to lead directly to core damage upon occurrence. For LOOP, a detailed ET-FT model was constructed to account for mitigation actions, including EDG start, auxiliary feedwater (AFW) supply, steam heat removal (SHR1, SHR2), and shutdown cooling (SDC) operation. The resulting high-wind PSA event tree is shown in Figure 1; of the 20 accident sequences, 16 were identified as leading to core damage (CD).

2.2. Intensity-based Dynamic Bayesian Network

Figure 2: ET-FT to BN Conversion Flowchart

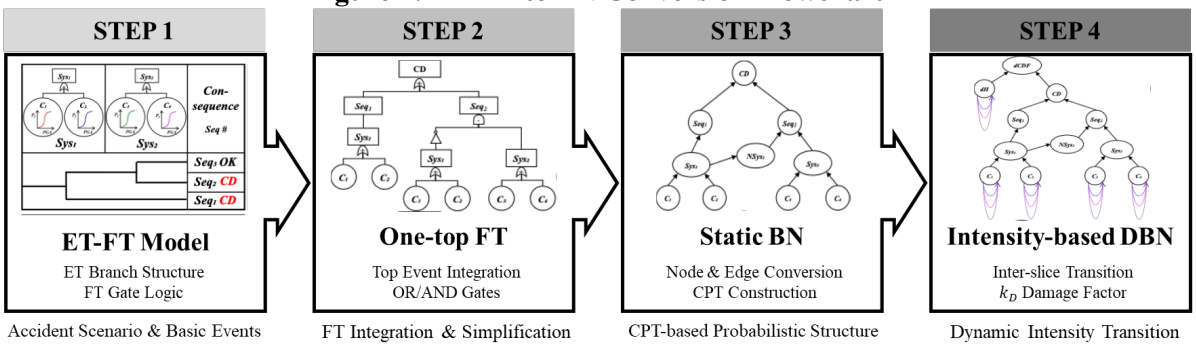

In this study, the ET-FT model is converted into a BN following the four-step procedure shown in Figure 2. First, a one-top FT is constructed by integrating each FT into a single top event, and the logic gate structure is converted into BN nodes and directed edges. The accident sequence branching structure of the ET is represented as CPTs, and OR and AND gates are reflected in the CPTs according to probability combination rules under the independence assumption. The mitigation systems for the LOOP initiating event (EDG, AFW, SHR, SDC) are represented as child nodes with the initiating event node as their parent, and the CD node is constructed as the top-level node integrating all accident sequences. Since a static BN represents the system state at a single point in time, it cannot capture the cumulative propagation of SSC damage states with increasing wind speed. To address this, this study proposes an intensity-based DBN in which the temporal index is reinterpreted as wind intensity level; the framework structure is shown in Figure 3. Fragility is defined as the probability that the limit state function G becomes negative given wind speed λ.

$$\boldsymbol{P_{f|\lambda} = P(G < 0 \mid \lambda)} \tag{1}$$

In practical evaluation, a lognormal distribution is assumed, expressed as follows.

$$\boldsymbol{P_f(V) = \Phi\left(\frac{\ln(V/V_m)}{\beta}\right)} \tag{2}$$

where V_m is the median capacity and β is the logarithmic standard deviation. If SSC damage occurs at a previous intensity level, the modified median capacity is calculated by applying the damage state factor $k_D \in (0,1]$.

$$\boldsymbol{V_m' = k_D \times V_m} \tag{3}$$

$k_D = 1.0$ corresponds to the undamaged baseline state, and the fragility increases as $k_D < 1.0$ with accumulated damage history. The modified fragility is expressed as follows.

$$\boldsymbol{P'_f(V) = \Phi\left(\frac{\ln\left(V/V'_m\right)}{\beta}\right)} \tag{4}$$

CCDP is obtained through BN inference at each intensity level, and CDF is calculated by convolving with the hazard curve $H(V)$.

$$\mathbf{CDF} = \sum_i \boldsymbol{dCDF_i} = \sum_i \mathbf{CCDP}_i \times \boldsymbol{\Delta H_i} \tag{5}$$

Figure 3: Intensity-Based DBN Framework for High Wind PSA

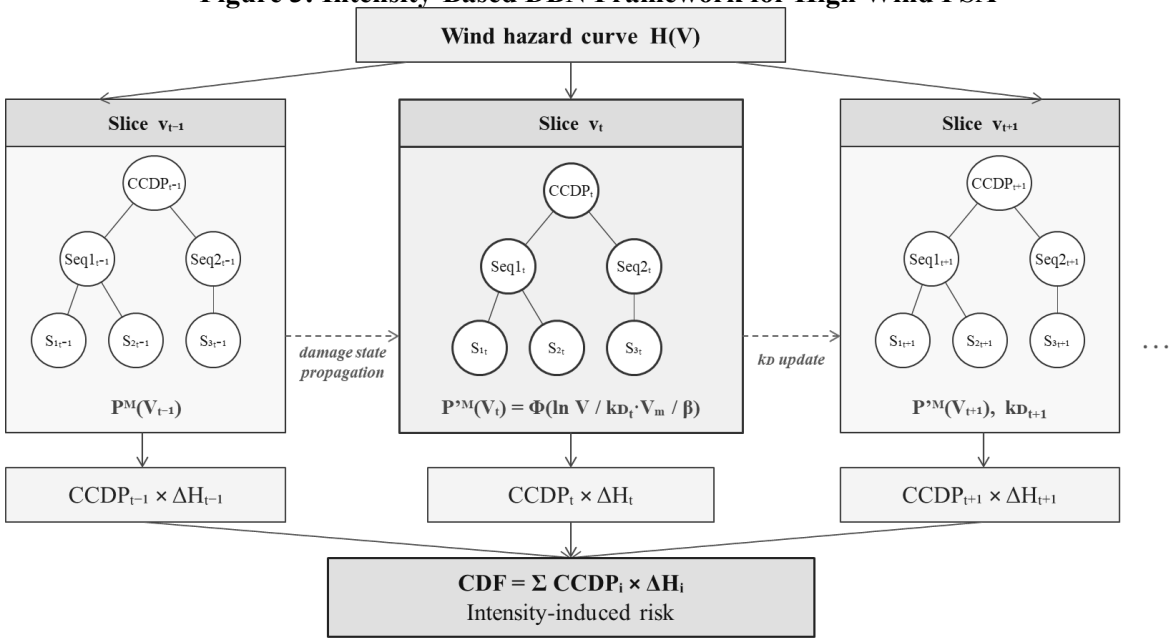

3. CASE STUDY

3.1. Case 1: Verification of DBN-Based High-Wind PSA Model

A DBN was constructed in GeNIe software based on the high-wind PSA ET-FT model developed in Section 2.1, and its structure is shown in Figure 4. The three initiating events considered are LEP, LOCCW, and LOOP, with the fragility and ET structure for each initiating event applied identically to Section 2.1. LEP and LOCCW are represented as OR gate structures of the AUX and EDGB, and ESW and CCW damage nodes, respectively, and LOOP is constructed as a composite structure including SWY and TB-related nodes. The mitigation systems for the LOOP initiating event (EDG, AFW, SHR1, SHR2, SDC, etc.) are represented as conditional probability nodes following the ET branching structure, and the CD node is constructed as the top-level node integrating all 16 CD accident sequences. The DBN consists of 6 intensity slices, and inference is performed in this section under the condition that no damage state factor (k_D) is applied. The fragility parameters applied to each SSC are listed in Table 1. The median capacity is calculated as $V_m = v_d\sqrt{F_s F_d F_p}$, where $v_d$is the design wind speed and F_s, F_d, $F_p$are the strength, ductility, and performance factors, respectively. The logarithmic standard deviation is defined as $\beta_c = \sqrt{\beta_r^2 + \beta_u^2}$, where $\beta_r$and $\beta_u$denote the randomness and uncertainty components, respectively, yielding β_c= 0.1414 for all SSCs. The appropriate values at the corresponding site were used for the hazard, and the ΔH_ivalues for each wind speed interval are given in Table 3. The wind

speed-dependent *CCDP* and *dCDF* results obtained from ET-FT and DBN analyses, respectively, are compared and summarized in Table 3.

Figure 4: Intensity-Based DBN Structure for High-Wind PSA Constructed in GeNIe

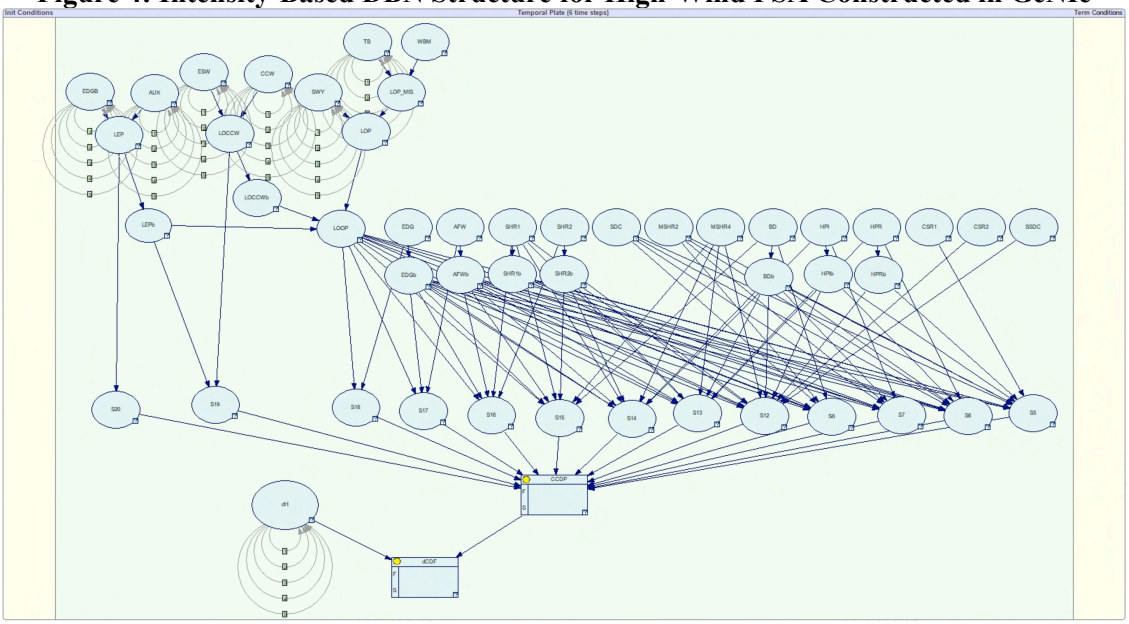

Table 1: Fragility Parameters for High Wind PSA SSCs

Component	$v_d(m/s)$	F_s	F_d	F_p	$V_m(m/s)$	β_r	β_u	β_c
EDGB	40	2.0	1.25	1.3	72.11	0.1	0.1	0.1414
AUX	40	2.0	1.25	1.3	72.11	0.1	0.1	0.1414
ESW	40	2.0	1.25	1.3	72.11	0.1	0.1	0.1414
CCW	40	2.0	1.25	1.3	72.11	0.1	0.1	0.1414
TB	40	2.0	1.25	1.3	72.11	0.1	0.1	0.1414
SWY	36.6	1.5	1	1	44.83	0.1	0.1	0.1414

Table 2: The *CCDP* by Wind Speed (ET-FT vs. DBN)

V(m/s)	$CCDP_{ET-FT}$	$CCDP_{DBN}$
35	2.13.E-05	1.76.E-05
40	1.70.E-04	1.51.E-04
45	1.97.E-03	1.92.E-03
50	1.95.E-02	1.93.E-02
55	1.07.E-01	1.04.E-01
60	3.35.E-01	3.07.E-01

Table 3: The *dCDF* by wind speed interval (ET-FT vs. DBN)

Interval (m/s)	$\Delta H_i(/yr)$	$dCDF_{ET-FT}(/yr)$	$dCDF_{DBN}(/yr)$
35–40	2.53.E-01	3.75.E-06	4.54.E-06
40–45	3.98.E-02	4.82.E-06	5.44.E-06
45–50	7.74.E-03	1.15.E-05	1.18.E-05
50–55	1.75.E-03	2.80.E-05	2.83.E-05
55–60	3.01.E-04	3.13.E-05	3.22.E-05
Total		7.94.E-05	8.23.E-05

Figure 5 shows the wind speed-dependent CCDP and interval-wise *dCDF* obtained from ET-FT analysis using MATLAB, and Figure 6 shows the DBN inference example results from GeNIe. The

results of the two methods were numerically consistent, confirming the validity of the DBN conversion for the full high-wind PSA scenario.

Figure 5: The *CCDP* and *dCDF* Results for High-Wind PSA using DBN

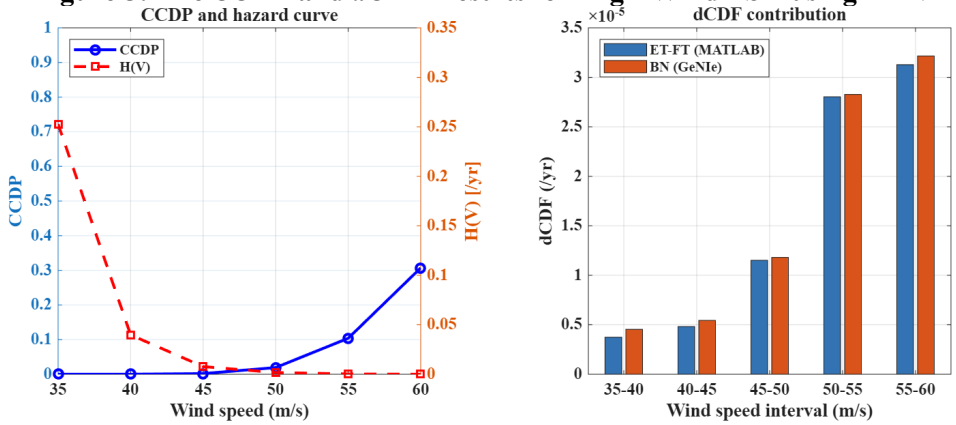

Figure 6: Intensity-Based DBN Inference Results for High-Wind PSA Obtained from GeNIe

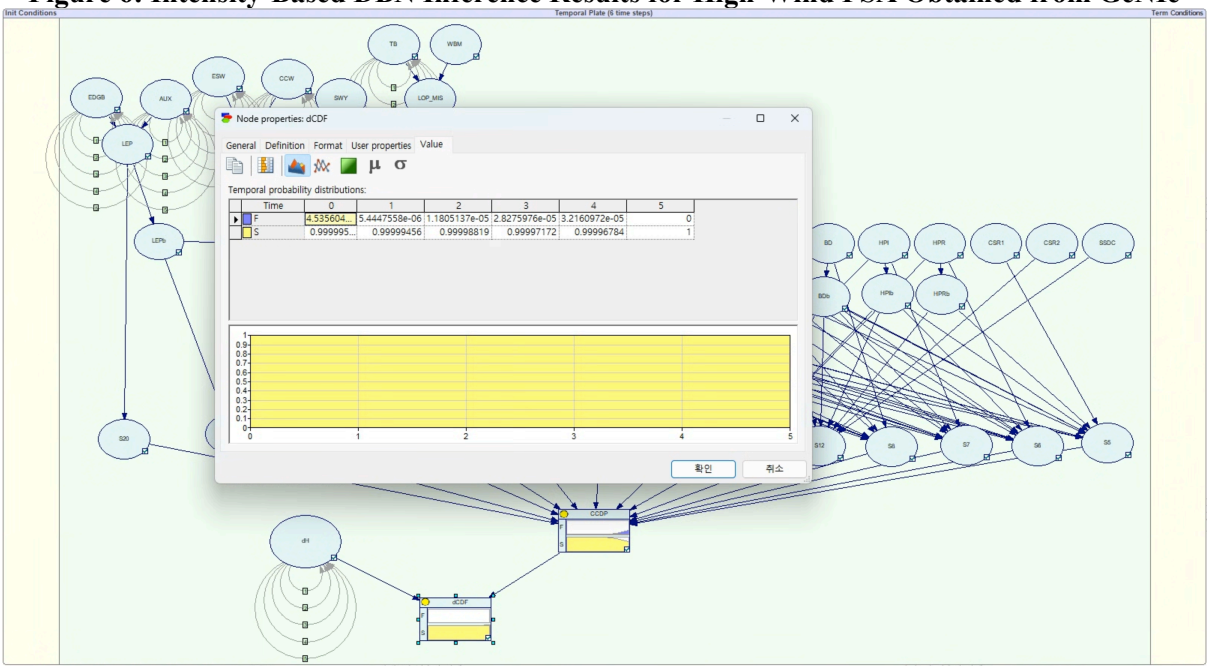

3.2. Case 2: Damage State Propagation Analysis Using Intensity-Based DBN

This section applies the intensity-based DBN framework proposed in Section 2.2 to analyze the change in risk at subsequent intensity levels when SSC damage occurs at a specific wind speed. The target scenario is the case in which EDGB is damaged at V= 50 m/s, and the modified fragility with damage state factor k_D= 0.9 is applied from the $V \geq 50$m/s interval onward. By comparing this with the undamaged baseline case (i.e., Case 1), the effect of damage history on system risk is quantitatively evaluated.

The two cases are defined as follows. Case 1 is the baseline case with k_D= 1.0 applied across all wind speed intervals, identical to the results of Section 3.1. Case 2 applies k_D= 0.9 to EDGB for $V \geq 50$m/s, updating the fragility with the modified median capacity $V_m' = k_D \times V_m$. The two cases are identical for $V <$ 50 m/s, and the CPT is updated from the interval following damage onset. The wind speed-dependent *CCDP* and *dCDF* results are summarized in Tables 4 and 5 and shown in Figure 7.

Table 4: The *CCDP* results: Case 1 (no damage) vs. Case 2 (EDGB k_D=0.9 at $V \geq 50$m/s)

V(m/s)	*CCDP* (Case 1)	*CCDP* (Case 2)
35	1.760E-02	1.760E-02
40	1.506E-01	1.506E-01
45	1.924E-01	1.924E-01
50	1.932E-02	4.641E-02
55	1.039E-01	1.855E-01
60	3.070E-01	4.342E-01

Table 5: The *dCDF* results: Case 1 (no damage) vs. Case 2 (EDGB k_D=0.9 at $V \geq 50$m/s)

Interval (m/s)	$\Delta H_i(/yr)$	*dCDF* (Case 1, /yr)	*dCDF* (Case 2, /yr)
35–40	2.130E-01	3.749E-06	3.749E-06
40–45	3.203E-02	4.824E-06	4.824E-06
45–50	5.987E-03	1.152E-05	1.152E-05
50–55	1.451E-03	2.803E-05	6.734E-05
55–60	3.012E-04	3.128E-05	5.586E-05
Total		**7.94E-05**	**1.43E-04**

As shown above, the *CCDP* and *dCDF* of the two cases are identical for V< 50 m/s, while the CCDP of Case 2 increases distinctly from the $V \geq 50$m/s interval onward. Specifically, in the 50–55 m/s interval, the CCDP increased from $1.93 \times 10^{-2}$to 4.64×10^{-2}, a factor of approximately 2.4, and in the 55–60 m/s interval, from $1.04 \times 10^{-1}$to 1.85×10^{-1}, a factor of approximately 1.8. The total CDF increased from 7.94×10^{-5}/yr of Case 1 to 1.43×10^{-4}/yr of Case 2, a factor of approximately 1.8. These results show that the SSC damage history at a previous intensity level has a significant effect on the fragility and system risk at subsequent intervals, and confirm that the damage state propagation effect, which cannot be represented by conventional static ET-FT models, can be explicitly modeled through the intensity-based DBN.

Figure 7: The *CCDP* and *dCDF* Comparison between Case 1 (No Damage) and Case 2 (EDGB k_D=0.9 at $V \geq 50$m/s)

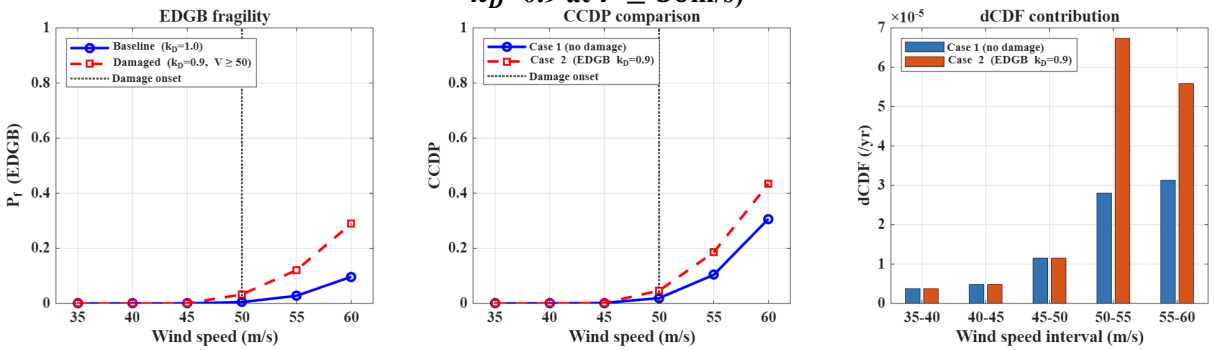

4. CONCLUSION

This study introduced an intensity-based DBN framework for high-wind external hazard PSA and tested its suitability for an OPR1000 reactor. The framework redefines the DBN's temporal index as a wind intensity level, allowing for SSC damage-state propagation with rising wind speeds and the calculation of intensity-resolved CDFs within a single, unified framework.

The results from the DBN inference aligned numerically with those based on ET-FT, confirming the validity of the DBN conversion. Using a damage state factor of k_D= 0.9 increased the overall CDF by about 1.8 times, showing that the DBN can explicitly account for damage history effects that traditional static models cannot capture. Future research will focus on applying real site data, expanding to multi-SSC damage scenarios, and conducting uncertainty propagation analysis.

Acknowledgements

This study was supported by the National Research Foundation of Korea (NRF) grant funded by the Korea government (Ministry of Science and ICT) (No. RS-2022-00144328). Also, this work was supported by the Nuclear Safety Research Program through the Korea Foundation of Nuclear Safety (KoFONS), granted financial resources from the Nuclear Safety and Security Commission (NSSC), Republic of Korea (RS-2024-00404119).

References

[1] IAEA. "*Consideration of External Hazards in Probabilistic Safety Assessment for Single Unit and Multi-unit Nuclear Power Plants*", Safety Reports Series No. 92, International Atomic Energy Agency, Vienna, (2017).
[2] ASME/ANS. "*Addenda to ASME/ANS RA-S-2008: Standard for Level 1/Large Early Release Frequency Probabilistic Risk Assessment for Nuclear Power Plant Applications*", ASME/ANS RA-Sa-2013, American Society of Mechanical Engineers/American Nuclear Society, New York, (2013).
[3] NISHINO, Hiroyuki, Hidemasa YAMANO, and Kenichi KURISAKA. "*Development of probabilistic risk assessment methodology against strong wind for sodium-cooled fast reactors*", Mechanical Engineering Journal, vol. 10, no. 4, p. 22-00387, (2023).
[4] G. Kim, S. Kwag, S. Eem, D. Hahm, and J. H. Park. "*Probabilistic safety assessment of off-site power system under typhoon considering failure correlation between transmission towers*", Reliability Engineering and System Safety, vol. 254, p. 110637, (2025).
[5] C. H. Phan, B. Won, S. Lee, and S. D. Kwon. "*Extreme wind-induced roof cladding failure: A fragility analysis for nuclear power plant structures*", Nuclear Engineering and Technology, p. 103928, (2025).
[6] S. Kwag and J. Oh. "*Development of network-based probabilistic safety assessment: A tool for risk analyst for nuclear facilities*", Progress in Nuclear Energy, vol. 110, pp. 178-190, (2019).
[7] J. D. Segarra, M. Bensi, and M. Modarres. "*A Bayesian network approach for modeling dependent seismic failures in a nuclear power plant probabilistic risk assessment*", Reliability Engineering & System Safety, vol. 213, pp. 107678, (2021).
[8] V. K. D. Mohan, P. H. van Gelder, P. Gehl, M. A. Hicks, and P. J. Vardon. "*Multi-hazard probabilistic safety assessments using Bayesian networks–A framework and demonstration for integrating technical and human risk*", Nuclear *Engineering and Design*, vol. 446, pp. 114558, (2026).
[9] E. Foerster, N. Girault, and A. Helminen. "*Probabilistic safety assessment for internal and external events on nuclear power plants and on mitigation strategies/H2020 European projects NARSIS, R2CA and BESEP*", EPJ N-Nuclear Sciences & Technologies, vol. 8, pp. 23, (2022).